PHASE TRANSITIONS IN V_2O_5 IN A HIGH RESOLUTION ELECTRON MICROSCOPE

H.J. FAN and L.D. MARKS

Center for Surface Radiation Damage Studies and Department of Materials Science and Engineering, Northwestern University, Evanston, Illinois 60208, USA

This paper presents data on phase transitions in vanadium pentoxide induced by electron beam irradiation in a high resolution electron microscope. The results show that the concentration gradient resulting from loss of oxygen from the surface drives a number of phase transitions. Two intermediate phases with orthorhombic structures, V_4O_9 and a modification of V_6O_{13}, were observed. The final product was a vanadium monoxide with a rock-salt-type structure. The end product and the intermediate phases have a well defined orientational relationship with the initial V_2O_5 phase, when the incident electron beam is along [001] or [110] of the V_2O_5. The average grain size of the final phase was proportional to the inverse square root of the flux of electrons, indicating diffusion-controlled nucleation.

1. Introduction

It is well known that many materials are damaged by ionizing radiation. Almost independent of the exact source of the ionizing radiation, single atoms or small molecules desorb from the surface. The original observations for many ionic solids [1–4] were ions, but more recent results have indicated that the main desorbants are neutrals or excited atoms [5–10]. In order to explain the desorption process induced by electron irradiation, many different damage mechanisms have been proposed [11,12]. One family of materials that has been extensively studied is the maximum valence transition metal oxides, i.e. oxides where the metal d shell is empty. High resolution electron microscopy is a valuable technique for studying electron-stimulated desorption processes from crystal surfaces at the atomic scale. In particular, most surface science techniques probe primarily the desorbants, so microscopic examination of what is left behind can complete the scientific picture. In the past few years the damage of a number of (primarily maximum valence) transition metal oxides has been investigated by these methods, see for instance refs. [13–21].

Damage of V_2O_5 induced by electron beam irradiation is an interesting research subject.

Vanadium pentoxide is an important catalyst and a maximum valence transition-metal oxide, having an orthorhombic structure with lattice parameters $a = 1.15$ nm, $b = 0.356$ nm and $c = 0.437$ nm. The V_2O_5 structure is built from a deformed octahedra with a longer, weak V–O bond along the c direction. Consequently, V_2O_5 is a layer structure with an (001) cleavage plane [22,23], and the oxygen atoms located at the cleavage plane might be easily lost during the electron beam irradiation. Enhancement of non-stoichiometry in the V_2O_5 crystal can be easily produced by various external stimulations such as heating, photon or electron bombardment. The decomposition of V_2O_5 to V_6O_{13} under low-energy electron bombardment has been investigated by Auger electron spectroscopy [24,25]. The reduction of vanadium pentoxide under the high-energy electron beam irradiation in an electron microscope has also been studied in-situ [26–28]. It was found that the final reduced phase is a metallic monoxide with rock-salt structure. Since damage is induced simultaneously by the electron beam through several mechanisms, the phase transition route and the final product depend on the experimental conditions and the prevailing mechanism.

In this paper we report the results of a detailed study of the reduction process of V_2O_5 crystal

under various accelerating voltages, electron beam irradiation fluxes and incident directions.

2. Experimental procedures

A powder of 99.9% pure V_2O_5 was ground in an alumina mortar and pestle while dispersed in methanol or acetone, then deposited on a holey carbon support film on a copper grid. The samples prepared for electron microscope observation were baked for about ten minutes on a light bulb in order to reduce surface hydrocarbon contaminants. These specimens were observed in a clean turbo-molecular-pumped Hitachi H-9000 high resolution electron microscope operated at 300 keV or 100 keV accelerating voltages in a vacuum of approximately 3×10^{-7} Torr.

The phase transitions were investigated by selected-area electron diffraction (SAED), high resolution electron microscopy (HREM) and surface profile imaging. A standard laser optical bench was used to obtain optical diffraction patterns from the high resolution electron micrographs corresponding to sample areas as small as 2000 $\AA^2$. The lattice spacings of the surface phase and the intermediate phases in some small areas can be accurately measured by reference to the diffraction pattern and the lattice fringes from the bulk V_2O_5. Samples with and without a carbonaceous contamination layer were observed at 300 keV accelerating voltage. It should be mentioned that we have repeated the experiments in a UHV HREM at 1.8×10^{-10} Torr and at 100 keV, and in both cases the results were essentially the same so we can rule out knock-on and vacuum effects.

3. Results and discussion

Figs. 1a–1e show a series of selected-area electron diffraction patterns of vanadium oxide irradiated by a low-flux beam of electrons at 300 keV. The first diffraction pattern (fig. 1a) was taken as soon as the crystal of vanadium pentoxide was tilted to the [001] orientation. Although structural changes cannot be seen from the diffraction pattern, the structure of the surface layer of V_2O_5 has

already changed. Fig. 2 is a high resolution image corresponding to the diffraction pattern in fig. 1a. A smaller square network of bright spots at the edge of the V_2O_5 crystal can be clearly seen. The distance between the bright spots corresponds to the d_{200} spacing of VO which has a rock-salt-type structure [16]. This phase extended rapidly from the surface of the crystal into the bulk at the rate of 1 nm/min under our experimental conditions.

Along the [001] orientation, the oxygen atoms were lost so rapidly at the surface of an irradiated crystal of V_2O_5 that no intermediate phases were observed at the surface. However, intermediate phases were observed in the bulk from SAED patterns (fig. 1b) and the corresponding HREM image (fig. 3) taken after ten minutes. It can be seen that there are four sets of extra diffraction spots due to two intermediate phases, V_4O_9, the twin of V_4O_9, a modification of V_6O_{13} (called m-V_6O_{13}) and the final phase VO, besides the main spots of V_2O_5. V_4O_9 has an orthorhombic structure with the lattice parameters $a = 0.824$ nm, $b = 1.003$ nm and $c = 1.65$ nm [29]. The twin-like diffraction patterns of V_4O_9 indicated by T and T' in fig. 1b result from different V_4O_9 domains as shown in fig. 3. The (110) plane of V_4O_9 at B_1 deviated by $-4°$ from the (100) plane of V_2O_5, and the (110) plane at B_2 deviated by $4°$ from the (100) plane of V_2O_5. Fig. 4 is a HREM image of V_2O_5, showing the intermediate phase V_4O_9. It can be seen from the areas A and B that V_4O_9 has a well defined orientational relationship with the parent phase V_2O_5,

$(110) V_4O_9 \parallel (100) V_2O_5$,

$(100) V_4O_9 \parallel (310) V_2O_5$,

$(001) V_4O_9 \parallel (001) V_2O_5$.
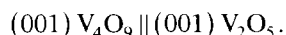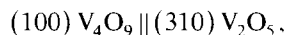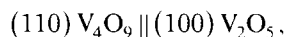
In fig. 4 each bright spot in the image of V_2O_5 corresponds to the center of an octahedron, i.e. the position of the vanadium atom. It can also be considered that the bright spots in V_4O_9 images represent the positions of the octahedra. It was noted that some of the bright spots were elongated along the direction indicated by the arrows, implying that there are minor movements of the vanadium and oxygen atoms from their initial lattice sites and a slight distortion of the V–O
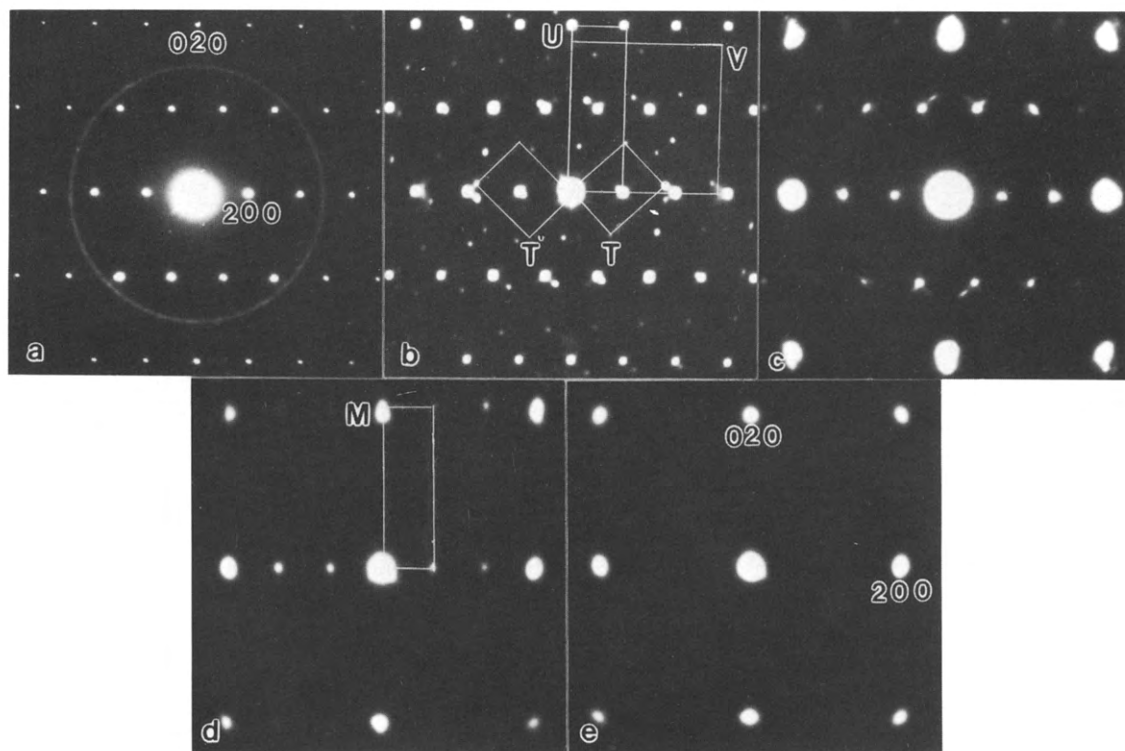
Fig. 1. SAED patterns from a crystal of vanadium oxide under electron beam irradiation: (a) [001] projection of the initial phase, V_2O_5; (b) intermediate phases V_4O_9 and m-V_6O_{13} which appeared after 10 min (the reciprocal unit cells of V_2O_5, V_4O_9 and VO are indicated by U, T, T' and V, respectively); (c) the intensity of the diffraction spots of m-V_6O_{13} and VO increased after 20 min; (d) SAED pattern of m-V_6O_{13} after 40 min; and (e) SAED of the end-product VO.
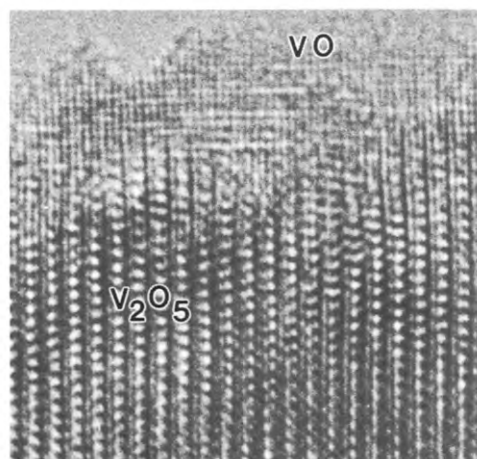

Fig. 2. HREM image from a crystal of V_2O_5 in the [001] projection showing that the structure has changed to VO at the surface.

octahedron. Comparing HREM images of both V_4O_9 and V_2O_5, we can conclude that V_4O_9 has a slightly distorted superstructure consisting of V_2O_5 with ordered oxygen vacancies. If one oxygen atom per unit cell of V_2O_5 is lost during electron beam irradiation, then the composition V_2O_5 would become that of V_4O_9. This is quite reasonable, since V_2O_5 can be transformed to V_4O_9 at lower temperatures in vacuum [30]. When the sample was irradiated by an intense electron beam, a number of strip-like V_4O_9 intergrowths were formed as shown in fig. 5. They were presumably induced by the vacancy density and nucleation rates increasing rapidly in these regions during irradiation (see later).

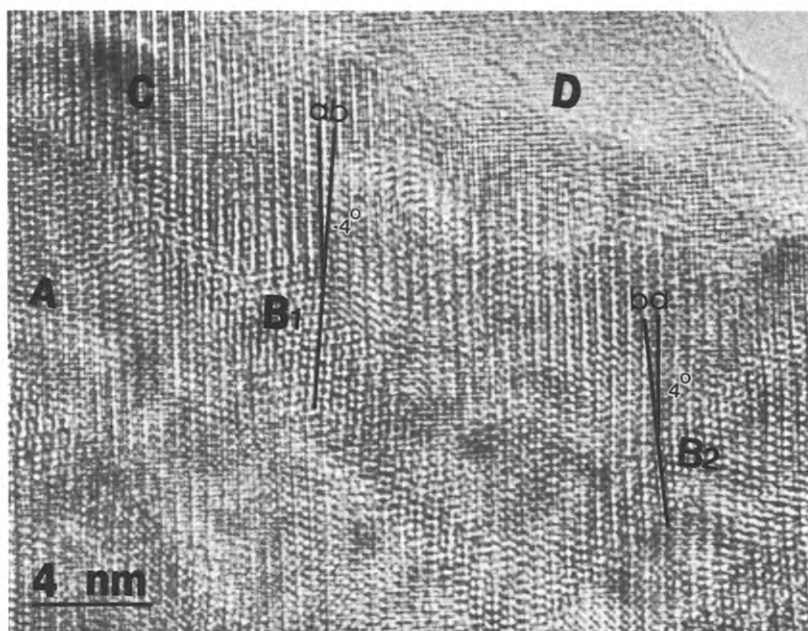Fig. 1c shows the electron diffraction pattern taken after 25 min irradiation. It can be seen that

Fig. 3. HREM image showing V_2O_5 transformed to V_4O_9 in area B and m-V_6O_{13} in area C.

the intensity of the m-V_6O_{13} and VO spots is enhanced and that of the V_4O_9 decreased. Fig. 1d is a diffraction pattern of the modification of V_6O_{13} taken after 40 min irradiation. The inter-planar distances measured from fig. 1d are 0.58 and 0.18 nm, slightly larger than the values of d_{200} and d_{020} for V_2O_5, and agree with the values of the d_{200} and d_{020} of V_6O_{13}. Tilting experiments
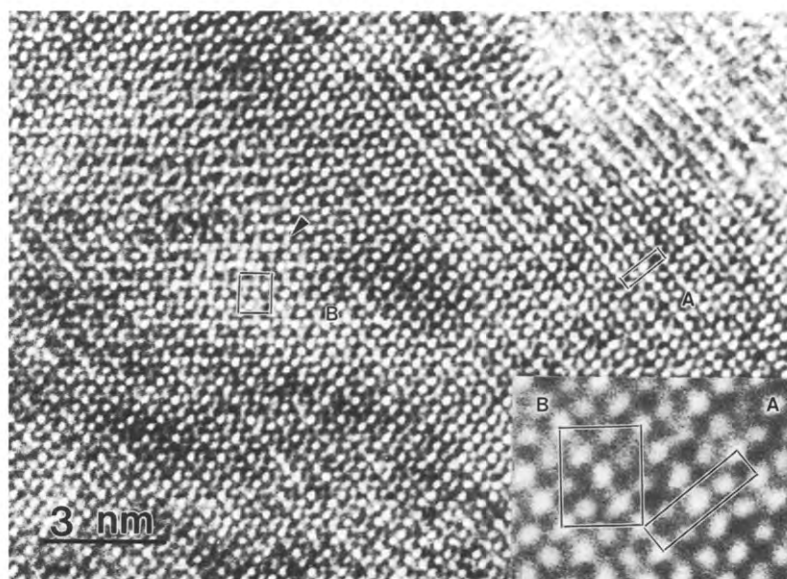

Fig. 4. HREM image showing a well defined orientation relationship between V_2O_5 and V_4O_9, with an enlarged image of area B (V_4O_9) and area A (V_2O_5) inset.
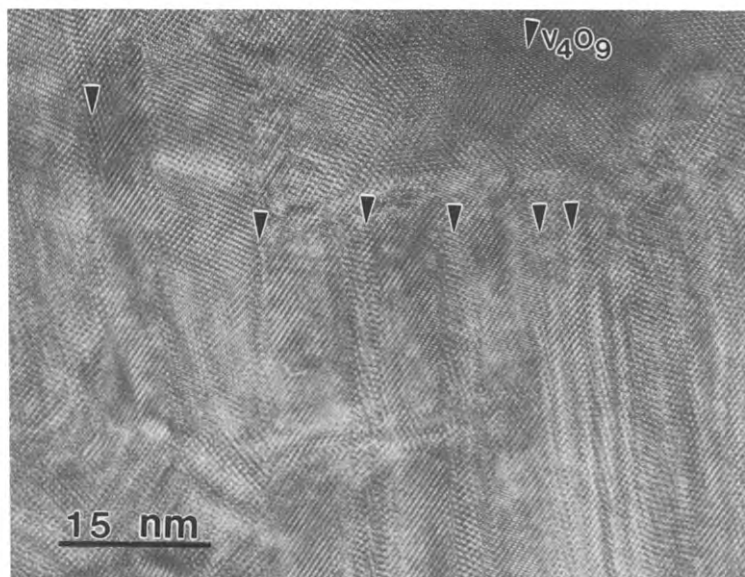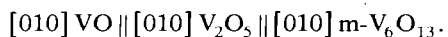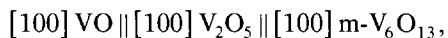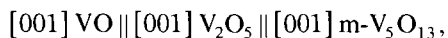
Fig. 5. Intergrowths of strip-like V_4O_9 with V_2O_5 which appeared under high-flux irradiation.

confirmed that this phase is orthorhombic. In addition, the HREM image and SAED pattern of the second intermediate phase show that the length of the a axis is approximately three times that of the a_0 axis of VO crystal, i.e. a triple superstructure of VO ($a = 3a_0$), or a modification of V_6O_{13}, called m-V_6O_{13} here.

Fig. 1e is an electron diffraction pattern of the final product after 1 h irradiation by the electron beam. Analysis of fig. 1e shows that this phase has a face-centered cubic structure with lattice parameter $a = 0.41$ nm. By comparing the data of the final product with all of the vanadium oxides, the final product was determined to be VO_{1-x}, where x is a small value, or VO for simplicity. The phase has a rock-salt-type structure with some disordered vacancies. The VO and m-V_6O_{13} crystals have a well defined epitaxial relationship with the parent V_2O_5:

$$[001] VO \parallel [001] V_2O_5 \parallel [001] m\text{-}V_5O_{13},$$

$$[100] VO \parallel [100] V_2O_5 \parallel [100] m\text{-}V_6O_{13},$$

$$[010] VO \parallel [010] V_2O_5 \parallel [010] m\text{-}V_6O_{13}.$$

No further changes were observed in the diffraction pattern of VO under continuous electron beam irradiation. This indicates that the end prod-

uct did not lose oxygen. Fig. 6 is a HREM image of the end product (VO) taken after 1 h irradiation with lower flux.

Fig. 7 shows the initial condition of a V_2O_5 crystal irradiated for 5 min with high flux. It can be seen that many smaller domains have formed, and the orientations of these domains are slightly different. In addition, the nonuniformity of the phase transition can be seen from the HREM
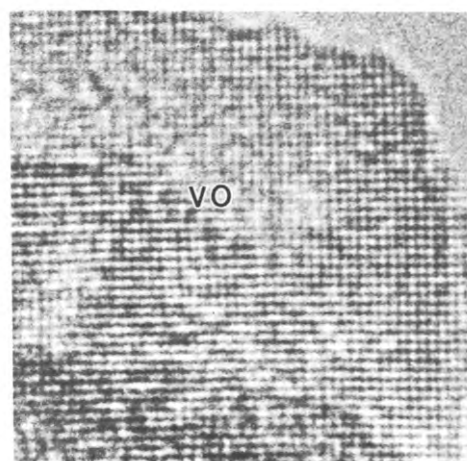

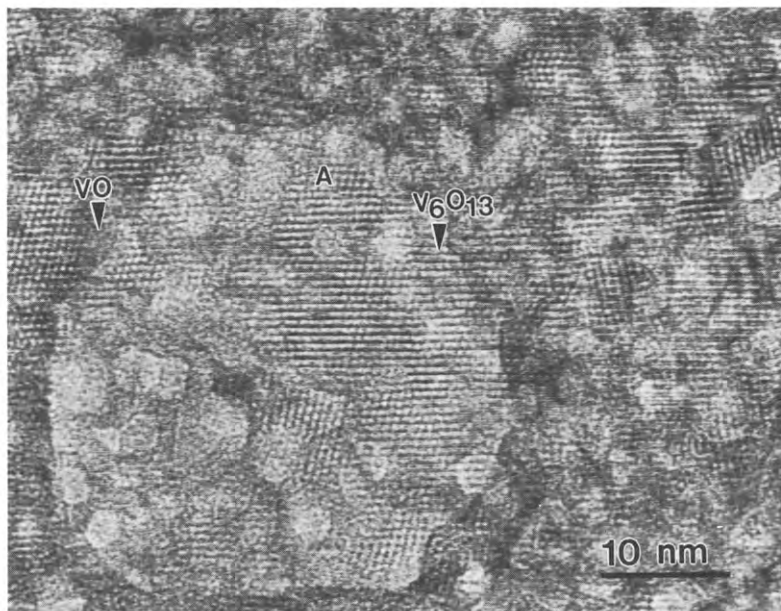Fig. 6. HREM image of the end-product VO after 1 h under low-flux irradiation.

Fig. 7. HREM image of V_2O_5 under high flux irradiation for 5 min, showing many smaller domains of different phases and overlap of both V_2O_5 and VO at area A.

image; some regions of V_2O_5 have been transformed to m-V_6O_{13} or VO phases, some areas have not. It is of interest that images of some bulk regions showed overlap of both V_2O_5 and VO (area A), indicating that the phase transition from V_2O_5 to VO was simultaneously occurring at the edge and top surface of the crystal.

It is found that the final grain size and the irradiation flux were directly related, as shown in fig. 8. The average grain size of the VO was inversely proportional to the square root of the irradiation flux as $D = C/F^{1/2}$, where D is the average grain size, F the irradiation flux, C a constant. This implies that the nucleation rate is proportional to the square root of the beam flux. If the dependence were linear, this could be understood as a homogeneous nucleation rate depending solely on the defect concentration. The fact that the dependence is square root indicates that the nucleation rate is diffusion controlled, with the effective diffusion constant proportional to the beam flux. Whether this is due to simply the dose dependence of the number of defects or a direct electron-stimulated diffusion is unclear, although we suspect the latter.

To sum up the above results, the overall phase transition route was:

$$V_2O_5 \rightarrow V_4O_9 \rightarrow m\text{-}V_6O_{13} \rightarrow VO,$$
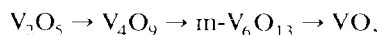
when the electron beam irradiation was along the [001] orientation of the V_2O_5 crystal. However, more detailed examination of the HREM images
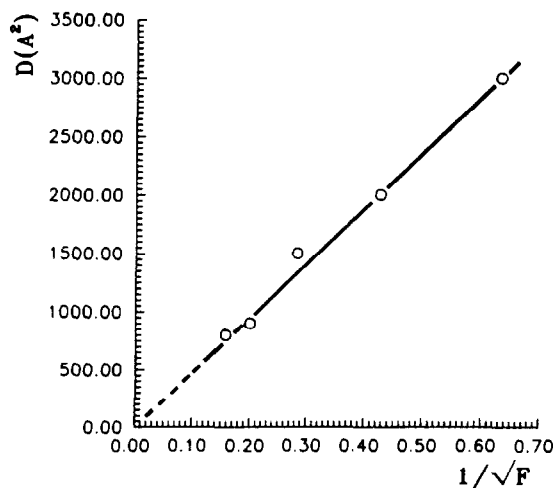

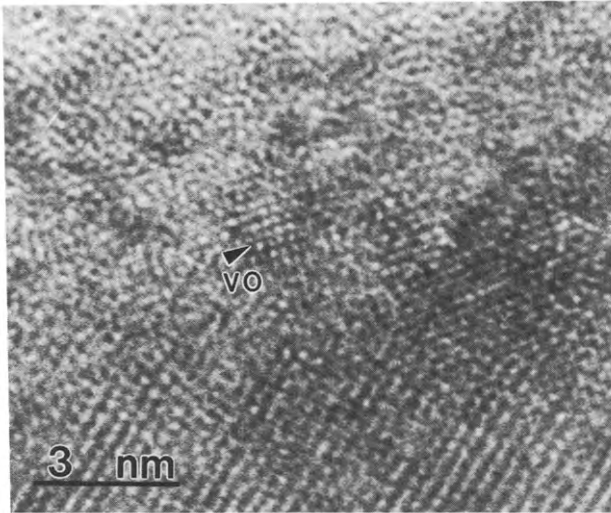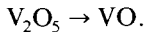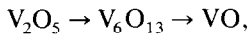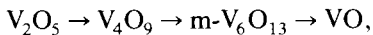Fig. 8. Dependence of average grain size on the electron flux.

Fig. 9. HREM image of V_2O_5 irradiated along the [101] orientation, showing VO and short-range-order structures formed at the surface.

shows that different mechanisms occur in different regions of the sample, and V_2O_5 phase was transformed directly to VO at the surface. The phase transition routes of the various regions were:

$$V_2O_5 \rightarrow V_4O_9 \rightarrow m\text{-}V_6O_{13} \rightarrow VO,$$

$$V_2O_5 \rightarrow V_6O_{13} \rightarrow VO,$$

$$V_2O_5 \rightarrow VO.$$

It should be noted that the same phase transitions were repeated at 100 kV accelerating voltage. This demonstrates that the predominant damage mechanism is electron-stimulated desorption (ESD) of oxygen rather than ballistic damage.

The same experiments were performed along other orientations of the V_2O_5 crystal. For irradiation along the [110] orientation, the end product of the phase transition was again VO, but the two intermediate phases, i.e. V_4O_9 and m-V_6O_{13}, were not observed.

Fig. 9 is a HREM image irradiated along the [101] orientation. It can be seen that a short-range-order structure was formed during the damage process. Crystallites of VO in the [101] orientation of about 200 Å^2 in size were formed at the areas indicated by arrows, without the intermediate phases of V_4O_9 and m-V_6O_{13}. It is ap-

parent that the phase transition process relates to the anisotropy of the crystal and the bonding.

4. Conclusions

The experimental results indicate the following conclusions:

(1) The initial desorption of oxygen atoms at the surface of the V_2O_5 crystal under electron beam irradiation can be explained by the Knotek–Feibelman mechanism (Auger decay process) or a similar mechanism, but this does not completely explain all the results. The concentration gradient induced by the desorption of oxygen at the surface drives oxygen diffusion from the bulk to the surface, which is the crucial physical process behind the phase transitions.

(2) Oxygen diffusion led to phase transitions in the bulk. The phases have a similar crystal system and a well defined epitaxial relationship with the parent phase.

(3) The irradiation damage depends on the crystal structure, the type of bond and the flux of the electron beam.

(4) For the same irradiation direction, the phase transition routes are different in different regions of the bulk, because there is a nonuniformity of the oxygen content due to different vacancy concentrations.

(5) The average grain size of final phase is proportional to the inverse square root of the beam flux, indicating that the nucleation rate depends on the defect concentration and is diffusion controlled.

References

[1] M.L. Knotek and P.J. Feibelman, Phys. Rev. Letters 40 (1987) 96.

[2] M.L. Knotek, Phys. Today, September (1984) 27.

[3] M.L. Knotek, Phys. Scripta T6 (1983) 94.

[4] M.L. Knotek and P.J. Feibelman, Surface Sci. 90 (1979) 78.

[5] P. Feulner, in: Desorption Induced by Electronic Transitions, DIET II, Eds. W. Brenig and D. Menzel (Springer, Berlin, 1984) p. 142.

[6] N.H. Tolk, R.F. Hagland, Jr., M.H. Mendenhall, E. Taglauer and N.G. Stoffel, in: Desorption Induced by Electronic Transitions, DIET II, Eds. W. Brenig and D. Menzel (Springer, Berlin, 1984) p. 152.

[7] R.F. Haglund Jr, R.G. Albridge, D.W. Cherry, R.K. Cole, M.H. Mendenhall, W.C.B. Peatman and N.H. Tolk, Nucl. Instr. Methods B 13 (1986) 525.

[8] N.H. Tolk, L.C. Feldman, J.S. Kraus, R.J. Morris, M.M. Traum and J.C. Tully, Phys. Rev. Letters 46 (1981) 134.

[9] N.H. Tolk, M.M. Traum, J.S. Kraus, T.R. Pian, W.E. Collins, N.G. Stoffel and G. Margaritondo, Phys. Rev. Letters 49 (1982) 812.

[10] P. Feulner, W. Riedl and D. Menzel, Phys. Rev. Letters 50 (1983) 986.

[11] See articles in: Desorption Induced by Electronic Transitions, DIET I, Eds. N.H. Tolk, M.M. Traum, J.C. Tully and T.E. Madey (Springer, Berlin, 1983).

[12] See articles in: Desorption Induced by Electronic Transitions, DIET II, Eds. W. Brenig and D. Menzel (Springer, Berlin, 1985).

[13] A.K. Petford, L.D. Marks and M. O'Keeffe, Surface Sci. 172 (1986) 496.

[14] L.D. Marks, D.J. Li, H. Shibahara and J.P. Zhang, J. Electron Microsc. Tech. 8 (1988) 297.

[15] D.J. Smith and L.A. Bursill, Ultramicroscopy 17 (1985) 387.

[16] D.J. Smith, M.R. McCartney and L.A. Bursill, Ultramicroscopy 23 (1987) 299.

[17] D.J. Smith, L.A. Bursill and D.A. Jefferson, Surface Sci. 175 (1986) 673.

[18] J.W. Strane, J.P. Zhang, B.W. Wessels and L.D. Marks, Surface Sci, submitted.

[19] L.A. Bursill, P.J. Lin and D.J. Smith, Ultramicroscopy 23 (1987) 223.

[20] J.W. Strane, L.D. Marks, D.E. Luzzi, M.I. Buckett, J.P. Zhang and B.W. Wessels, Ultramicroscopy 25 (1988) 253.

[21] A.K. Petford-Long and D.J. Smith, Phil. Mag. 54 (1986) 837.

[22] A. Bystrom, K.A. Wilhelmi and D. Brotzen, Acta Chem. Scand. (1950) 1119.

[23] H.G. Bachmann, F.R. Ahmed and W.H. Barnes, Z. Krist. 115 (1961) 110.

[24] M.N. Colpaert, P. Clauws, L. Fiermans and J. Vennik, Surface Sci. 36 (1973) 513.

[25] I.M. Curelaru, Solid State Commun. 34 (1980) 729.

[26] T. Ohno, Y. Nakamura and S. Nagakura, J. Solid State Chem. 56 (1985) 318.

[27] R.J.D. Tilley and B.G. Hyde, J. Phys. Chem. Solids 31 (1970) 1613.

[28] K.A. Wilhelmiand and K. Waltersson, Acta Chem. Scand. 24 (1970) 3409.

[29] F. Theobald, R. Cabala and J. Bernard, Compt. Rend. Acad. Sci. 269c (1969) 1209.

[30] G. Grymonprez, L. Fiermans and J. Vennik, Acta Cryst. A 33 (1977) 834.